

Opposing Effects of PKC θ and WASp on Symmetry Breaking and Relocation of the Immunological Synapse

Tasha N. Sims,^{1,6} Timothy J. Soos,¹ Harry S. Xenias,³ Benjamin Dubin-Thaler,³ Jake M. Hofman,⁴ Janelle C. Waite,¹ Thomas O. Cameron,¹ V. Kaye Thomas,¹ Rajat Varma,¹ Chris H. Wiggins,⁵ Michael P. Sheetz,³ Dan R. Littman,^{1,2} and Michael L. Dustin^{1,*}

¹ Molecular Pathogenesis Program, Skirball Institute of Biomolecular Medicine, New York University School of Medicine, New York, NY 10016, USA

² Howard Hughes Medical Institute and Skirball Institute of Biomolecular Medicine, New York University School of Medicine, New York, NY 10016, USA

³ Department of Biological Sciences

⁴ Department of Physics

⁵ Department of Applied Physics and Applied Mathematics
Columbia University, New York, NY 10027, USA

⁶ Present address: Regeneron Pharmaceuticals, Inc., Tarrytown, NY 10591, USA.

*Correspondence: dustin@saturn.med.nyu.edu

DOI 10.1016/j.cell.2007.03.037

SUMMARY

The immunological synapse (IS) is a junction between the T cell and antigen-presenting cell and is composed of supramolecular activation clusters (SMACs). No studies have been published on naive T cell IS dynamics. Here, we find that IS formation during antigen recognition comprises cycles of stable IS formation and autonomous naive T cell migration. The migration phase is driven by PKC θ , which is localized to the F-actin-dependent peripheral (p)SMAC. PKC $\theta^{-/-}$ T cells formed hyperstable IS in vitro and in vivo and, like WT cells, displayed fast oscillations in the distal SMAC, but they showed reduced slow oscillations in pSMAC integrity. IS reformation is driven by the Wiscott Aldrich Syndrome protein (WASp). WASp $^{-/-}$ T cells displayed normal IS formation but were unable to reform IS after migration unless PKC θ was inhibited. Thus, opposing effects of PKC θ and WASp control IS stability through pSMAC symmetry breaking and reformation.

INTRODUCTION

T cells require an intact actin cytoskeleton to initiate T cell receptor (TCR) clustering and signaling (Valitutti et al., 1995; Varma et al., 2006). F-actin may regulate the diffusion, followed by the trapping process, that brings signaling molecules to TCR clusters (Douglass and Vale, 2005). Signaling downstream of the TCR triggers production of dynamic F-actin, thus creating a potential positive-feedback

loop (Bubeck Wardenburg et al., 1998). Antigen recognition also requires adhesion molecules, and many are F-actin dependent (Kucik et al., 1996). Finally, T cells contact antigen-presenting cells through a process of stochastic repertoire scanning, an active search that uses F-actin-dependent amoeboid locomotion (Miller et al., 2003).

T cells' rapid locomotion that characterizes the search for antigen gives way to a period of stable T cell interaction once antigen recognition takes place (Mempel et al., 2004; Okada et al., 2005). This stable phase is consistent with immunological synapses (ISs) that have been studied extensively in vitro with antigen-experienced T cells or clones and antigen presentation by B cells or supported planar bilayers containing MHC-peptide complexes and adhesion ligands (Grakoui et al., 1999; Monks et al., 1998). The IS is a radially symmetrical structure with three major compartments referred to as SMACs (Monks et al., 1998). The central SMAC (cSMAC) was initially described as a signaling structure (Freiberg et al., 2002; Monks et al., 1998), but this zone may primarily carry out endocytic and exocytic processes linked to TCR degradation and directed secretion (Stinchcombe et al., 2006; Varma et al., 2006). Laterally outward from the center is the peripheral SMAC (pSMAC), a ring of LFA-1/ICAM-1 interactions colocalized with the cytoskeletal integrin linker talin (Monks et al., 1998). Continuing outward to the edge of the IS is the distal SMAC (dSMAC), a zone enriched in the tyrosine phosphatase CD45 (Freiberg et al., 2002). Structures that sustain TCR signaling have recently been identified: TCR microclusters form in the dSMAC and continually translocate through the pSMAC to the cSMAC (Varma et al., 2006).

Adaptive immune recognition evolved in early vertebrates, whereas mechanisms of F-actin and myosin-based amoeboid mobility evolved in motile single-cell organisms such as dictyostelium. Evolution of specialized recognition

mechanisms such as the IS may utilize common machinery of mobile cells. The basic engine for amoeboid locomotion is protrusion that is driven by F-actin polymerization and linked to F-actin and myosin-II-based contraction (Lin et al., 1996). Linkage of adhesion molecules to the F-actin network during polarized protrusion and the maintenance of these linkages during contraction lead to forward motion at up to 30 $\mu\text{m}/\text{min}$, and further contraction at the back of the cell leads to release of substrate interactions (Pollard and Borisy, 2003). The leading edge is a sensory structure defined as a lamellipodium that uses actin-based protrusion and myosin-II-based contraction to test the substrate (Giannone et al., 2004). The lamellipodium oscillates at >1 cycle per minute, and this oscillation can take the form of circular waves during cell spreading. Diverse cell types including insect cells, human fibroblasts, and mouse lymphocytes display this dynamic character (Dobereiner et al., 2006). Traction forces for movement are generated in the more stable lamella (Gupton et al., 2005), which has also been referred to as an asymmetric focal zone (Smith et al., 2005). Talin is a marker of the lamella, the focal zone and the pSMAC, suggesting a possible relationship between these structures (Gupton et al., 2005; Monks et al., 1998; Smith et al., 2005). The radial symmetry of the IS and particularly the pSMAC may account for positional stability, and reinstating T cell migration would require symmetry breaking (Verkhovskiy et al., 1999).

Protein kinase C- θ (PKC θ), a member of the “novel” PKC subfamily, is the only PKC isoform that redistributes to the IS (Monks et al., 1997). PKC θ is localized in the cSMAC or pSMAC (Monks et al., 1998; Sanchez-Lockhart et al., 2004; Somersalo et al., 2004). PKC θ is required for NF κ B, NF-AT, and AP-1 activation, IL2 production, and Th2 differentiation (Berg-Brown et al., 2004; Marsland et al., 2004; Sun et al., 2000). PKC θ may also be involved in pathways connecting TCR to the actin cytoskeleton (Thome, 2003; Villalba et al., 2002), perhaps via events mediated through WASp interacting protein (WIP) (Krzewski et al., 2006; Sasahara et al., 2002). The role of PKC θ in the regulation of IS dynamics is not known.

WASp is a regulator of the Arp2/3 complex that plays a critical role in formation of specialized adhesive junctions in the myeloid lineage (Calle et al., 2004) and antagonizes the PKC θ -dependent formation of WIP-myosin II complexes (Krzewski et al., 2006). T cells from WASp-deficient mice have defects in IL2 production (Snapper et al., 1998). Human CD4 $^+$ T cells from WAS patients had defects in the production of Th1 but not Th2 cytokines (Trifari et al., 2006). WIP binds to and stabilizes WASp in the resting state, and the complex is separated upon cell activation (Sasahara et al., 2002). The impact of WASp deficiency on IS formation is not clear: One study found defects in WASp-deficient T cells (Badour et al., 2003), whereas another group found normal IS formation (Cannon and Burkhardt, 2004).

Here, we examine the genetic control of IS stability. We find that neither PKC θ nor WASp is required for formation of the IS. PKC θ is required for the periodic symmetry

breaking in the contact leading to short bursts of mobility during early phases of antigen recognition. WASp, on the other hand, is needed to re-establish symmetry. Thus, PKC θ and WASp play opposing roles in balancing symmetry breaking and generation to regulate dynamics of early T cell priming.

RESULTS

PKC- θ Is Localized in the pSMAC on Supported Planar Bilayers

We wanted to determine whether the SMACs as defined for activated T cells interacting with B cells (Freiberg et al., 2002) can be directly related to zones formed by naive T cells interacting with supported planar bilayers containing ICAM-1, CD80, and agonist MHC-peptide complexes (Bromley et al., 2001). We fixed AND TCR Tg T cells after 45 min of interaction with the bilayer, performed fluorescence staining for CD45 (dSMAC), talin (pSMAC), and TCR (cSMAC) (Figure 1A), and used total internal reflection fluorescence microscopy (TIRFM) to focus on cellular signals within 200 nm of the planar bilayer (Varma et al., 2006). Phalloidin staining detected F-actin. CD45 was most brightly stained in an approximately 1- to 2- μm -thick ring that was also stained brightly with phalloidin (Figure 1B), consistent with a dSMAC. Talin stained an intermediate ring of ~ 2 μm thickness, and this ring had relatively less CD45 and phalloidin staining (Figure 1B), consistent with a pSMAC. The TCR stained most strongly in a bright central cluster (Figure 1B), consistent with a cSMAC. Peripheral TCR microclusters are faintly visible in the images (yellow arrow). ICAM-1 accumulation in the bilayer was strongest in the pSMAC zone (Figure 1B), consistent with earlier studies. The dSMAC as marked by CD45 can also be located in images of ICAM-1 accumulation as an area that is outside the pSMAC and that often shows exclusion of ICAM-1 (white arrow). Thus, we used ICAM-1 accumulation as a marker of the pSMAC. We examined the location of PKC θ in fixed IS by using a polyclonal affinity-purified antibody. PKC θ accumulated in the pSMAC zone in 60% of contacts and at the junction between the dSMAC and pSMAC zones in 35% of IS by TIRFM (Figure 1C). PKC θ staining was localized in small punctae (arrows) in the ICAM-1 region but did not precisely overlay the ICAM-1 accumulations. IS formed here with CD80 incorporated in the bilayer differed from earlier results with B cells or fibroblasts expressing CD80, where PKC θ staining was found to be a marker of the cSMAC (Monks et al., 1998; Sanchez-Lockhart et al., 2004). We did not detect a signal in PKC θ -deficient T cells by using the PKC θ antisera (Figure S1 in the Supplemental Data available with this article online). We tested the dependence of the pSMAC on F-actin by treating IS with 1 μM latrunculin A, an inhibitor of actin polymerization. ICAM-1 accumulation decreased in intensity and became more dispersed in the interface within 2 min of latrunculin A treatment, whereas the central accumulation of TCR remained intact (Figure 1D). Washing latrunculin A from the

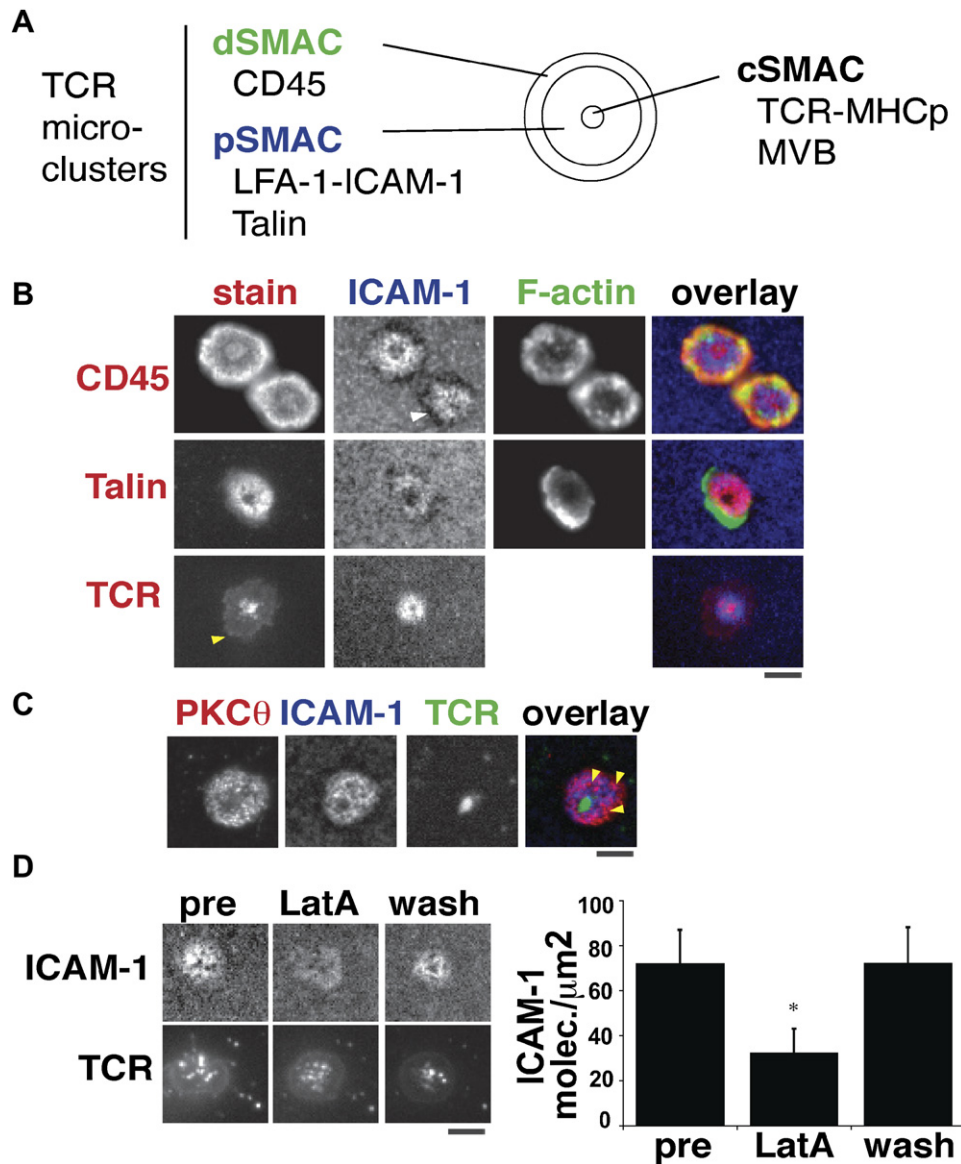


Figure 1. Primary T Cell Cytoskeletal Regions and Actin Dependence

(A) Schematic of markers of SMAC regions of the T cell IS. MVB stands for multi-vesicular bodies.

(B–D) Naive AND T cells were adhered to bilayers containing ICAM-1, CD80, and MHC-peptide complexes. The interface of T cells contacting the bilayer was imaged by TIRFM. Scale bars represent 4 μm (B) shows representative staining of markers of SMAC regions of the naive T cell IS. Cells were fixed at 45 min, permeabilized, and stained for F-actin and regional markers. TCR images are from a live cell at 40 min. (C) shows PKCθ staining. Naive AND T cells were adhered to bilayers, fixed at 50 min, permeabilized, stained for PKCθ and TCR, and imaged by TIRFM. (D) shows naive AND T cells that were stained with monovalent Fabs to TCR, adhered for 20 min to bilayers, and imaged by wide-field microscopy. Cells were treated with 1 μM latrunculin A for 10 min., imaged, washed, and then reimaged. Left panels show representative images. The graph on the right side shows quantification of ICAM-1 molecules in the contact (Grakoui et al., 1999); averages and SD are shown. *t test, $p < 0.0001$. All images are representative of at least three experiments.

cells restored strong ICAM-1 accumulation in the pSMAC after 5 min (Figure 1D). Treatment with the microtubule disruptor colchicine had no effect on the intensity of ICAM-1 accumulation in the pSMAC over 30 min, although it did destroy the microtubule network (data not shown). Thus, PKCθ is accumulated in the F-actin-dependent pSMAC in naive T cells interacting with supported planar bilayers

presenting agonist MHC-peptide complexes, adhesion, and costimulation signals.

PKCθ Is Not Required to Form the IS

We next determined whether PKCθ is required for IS formation. Naive T cells from AND TCR Tg PKCθ^{-/-}, PKCθ^{+/-}, or PKCθ^{+/+} formed nearly identical IS on planar

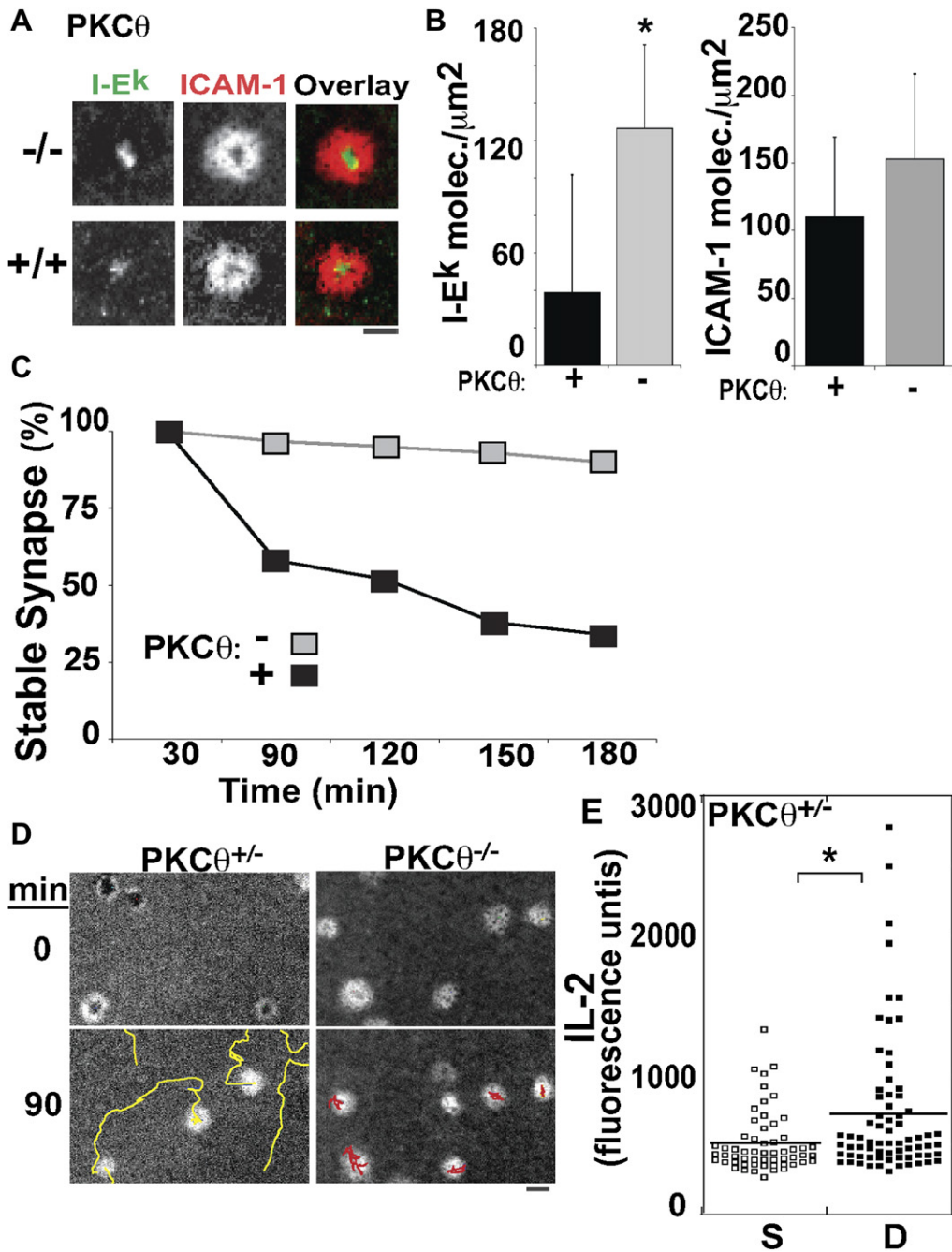


Figure 2. PKC θ Destabilizes the IS and Promotes Smaller cSMAC Size

(A and B) PKC $\theta^{-/-}$ T cells form IS on bilayers containing agonist MHC-peptide complexes, CD80, and ICAM-1. (A) shows naive CD4 $^{+}$ T cells that were purified from littermate AND PKC $\theta^{-/-}$ or PKC $\theta^{+/+}$ mice. Images were acquired at 20 min. The experiment was repeated at least eight times, as well as performed with 5CC7 and 2B4 TCR transgenic PKC $\theta^{-/-}$ and PKC $\theta^{+/+}$ T cells, and showed similar results. (B) shows that I-Ek (cSMAC) and ICAM-1 (pSMAC) density accumulated in the IS to 40 min was quantified (20 PKC $\theta^{+/+}$ and 37 PKC $\theta^{-/-}$ cells measured). Data are representative of two independent experiments. Averages and SD are shown. *t test, $p < 0.0001$. The scale bar represents 4 μm .

(C) PKC θ destabilizes IS in vitro. The percentage of stable IS was plotted for each genotype over time. Differences between PKC $\theta^{-/-}$ and PKC $\theta^{+/+}$ are statistically significant by χ^2 , $p < 0.001$. The representative time course of at least six similar experiments is shown.

(D) Representative AND T cell travel during 90 min time course. The center of the IS was marked (0 min), and lines show cells' paths over 90 min. ICAM-1 planar bilayer images are shown. The scale bar represents 4 μm .

(E) Destabilized IS promote IL-2 secretion. Representative AND T cell IL-2 secretion plots at 6 hr for stable (S) and destabilized (D) IS. More than 200 cells were analyzed in each category. The error bar represents averages. *Mann-Whitney U, $p = 0.002$.

Table 1. Comparison of Dynamic IS Interactions

	IS (%)	Stable IS (%)	IS Duration (min)	Move (%)	Move and Reform IS (%)	Movement Duration (min)	Average Speed ($\mu\text{m}/\text{min}$)	Average Polarity (μm)
Wild-type	67	22	17 \pm 31	78	90	35 \pm 20	0.36	1.33
PKC $\theta^{-/-}$	40	85 ^a	83 \pm 29 ^b	15	9 ^a	5 \pm 3 ^c	0.002 ^b	0.66 ^b
WASp $^{-/-}$	80	3	12 \pm 5	97	17	ND	0.89 ^b	2.72 ^b

Quantification of time-lapse fluorescence imaging of naive WT, PKC $\theta^{-/-}$, and WASp $^{-/-}$ AND TCR Tg T cells interacting with bilayers containing ICAM-1-Cy5, I-E^k, and CD80 over 95 min (to 45 min for WASp $^{-/-}$). ND stands for “not determined,” and durations represent averages \pm SD.

^aChi square compared to WT, $p < 0.01$.

^bResults from t test compared to WT, $p < 0.0001$.

^cResults from t test compared to WT, $p = 0.006$.

bilayers (Figure 2A and Figure S2A). PKC $\theta^{-/-}$ T cells accumulated greater amounts of MHCp complexes in the cSMAC than PKC $\theta^{+/+}$ cells (Figure 2B) but had similar levels of ICAM-1 accumulated in the pSMAC at 30 min (Figure 2B). When PKC θ -YFP was introduced into naive PKC $\theta^{-/-}$ T cells by electroporation, the YFP signal was concentrated in the pSMAC region, thus confirming the localization reported by the PKC θ -specific antibody (Figure S2B). Thus, PKC θ is not required for IS formation. The significance of a larger cSMAC was not immediately clear, so the dynamics of IS formed by naive PKC $\theta^{+/+}$ and PKC $\theta^{-/-}$ T cells was studied further.

PKC θ Is Required for pSMAC Symmetry Breaking

To evaluate IS dynamics, we first performed an IS-survival analysis by starting with T cells that formed IS on bilayers by 30 min and following their location over the next 180 min with the rule that the IS survived if the cell moved less than 10 μm (i.e., one cell diameter) from its original location. To our surprise, only 30% of naive PKC θ -expressing T cells' ISs survived for 180 min, with a half-life of 90 min. In contrast, 88% of PKC $\theta^{-/-}$ T cell IS survived for 180 min with an extrapolated half-life of \sim 10 hr (Figure 2C). Time-lapse analysis of ICAM-1-accumulation images revealed that PKC θ -expressing cells periodically broke open the pSMAC to create an asymmetric focal-zone accumulation pattern and relocated to nearby areas, where the pSMAC reformed (Table 1 and Figure 2D; see also Movies S1 and S2 and Figure S2C). The relocation process, which has a periodicity of \sim 20–40 min, is autonomous because the cells are interacting with a homogeneous substrate free of gradients in MHCp, CD80, or ICAM-1, without chemotactic gradient imposed. Remarkably, PKC $\theta^{-/-}$ T cells did not relocate and displayed less marked symmetry breaking of the pSMAC over several hours (Table 1 (polarity) and Figure 2D; see also Movies S3 and S4). We did not observe differences between PKC $\theta^{+/+}$ and PKC $\theta^{+/-}$ T cells in IS formation or symmetry breaking (data not shown). Because naive T cells do not spread on ICAM-1 alone, we were unable to test the role of PKC θ in antigen-independent migration in vitro. Expression of PKC θ -YFP in PKC $\theta^{-/-}$ naive T cells resulted in increased observation of pSMAC breaking: 10 of 11 YFP-

positive cells in two experiments had lost pSMAC symmetry within 40 min, a similar time course as WT cells. Because PKC θ expressing T cells contained a minority of cells that formed continuously symmetrical pSMAC over the 6 hr period required to assess IL2 production, we compared IL2 release from stable versus relocated IS. Interestingly, T cells that relocated their ISs at least once during this period made significantly more IL2 than cells that remained within one cell diameter of their earlier location (Figure 2E, $p = 0.002$). Together, these data indicate that naive T cells periodically break and reform the pSMAC in a PKC θ -dependent manner and relocate via a transient LFA-1/ICAM-1 focal zone. This cycle of IS formation, migration, and IS relocation is correlated with greater IL2 production.

PKC θ Promotes T Cell Motility during Antigen Recognition In Vivo

We next tested for physiological changes in T-DC (dendritic cell) interaction stability with and without PKC θ in vivo by using confocal intravital microscopy. In vivo, T cells search for antigen by migrating actively within DC networks (Lindquist et al., 2004) and slow their migration for a period of hours after encounters with antigen-expressing DC (Mempel et al., 2004). We imaged T cell dynamics in the DC-rich spleen (Kraal et al., 1986), an important location for T cell responses, by intravital confocal microscopy (Sevilla et al., 2003). The advantage of the splenic red pulp is that T cells migrate over sessile DC networks 30 μm under the capsule (Figure S3A). We labeled PKC $\theta^{+/+}$ and PKC $\theta^{-/-}$ DO11.10 TCR transgenic T cells with different fluorescent dyes and transferred them into background-matched WT recipients (Figure S3B). Baseline migration (without exogenous antigen) of PKC $\theta^{+/+}$ and PKC $\theta^{-/-}$ DO11.10 T cells was similar (Mann-Whitney U, $p = 0.49$) (Movie S5). We synchronously activated all DO11.10 T cells in the spleen by i.v. ovalbumin-peptide injection (Zell et al., 2001) and determined both T cell speed and displacement. Although this would be a tolerogenic stimulus, we previously found that the stability of T-DC interactions is similar for CD4⁺ T cells under conditions of tolerance induction and immunization (Shakhar et al., 2005). We scored arrest as T cell movement of $<20 \mu\text{m}$

from the initial position during an imaging period of 60 min. In response to antigen in the spleen, we observed three phases of T cell movement: early transient interactions, intermediate arrest, and a late phase of high mobility similar to phases observed in the lymph node (Mempel et al., 2004). Ovalbumin peptide had little effect on migration of PKC $\theta^{+/+}$ or PKC $\theta^{-/-}$ DO11.10 T cells in the first 2 hr (data not shown). Antigen-induced arrest of both PKC $\theta^{+/+}$ and PKC $\theta^{-/-}$ DO11.10 T cells was maximal at 3–8 hr, but significantly fewer PKC $\theta^{+/+}$ T cells arrested compared PKC $\theta^{-/-}$ T cells (Figure 3A and Movie S6). Detailed analysis of migration speed showed that the distribution is shifted to faster speeds for the PKC $\theta^{+/+}$ DO11.10 T cells compared to PKC $\theta^{-/-}$ DO11.10 T cells (Figure 3B). Both PKC $\theta^{+/+}$ and PKC $\theta^{-/-}$ DO11.10 T cells resumed migration by 16 hr after ovalbumin-peptide injection (Figure 3A). Non-TCR transgenic PKC $\theta^{+/+}$ T cells did not change stopping, migration speed, or displacement between 3 and 16 hr (Figure 3A; see also Figure S4 and Movies S7 and S8). We conclude that PKC θ induces relocation of T cell IS in vitro and decreases arrest in vivo but that PKC θ is dispensable for surveillance of DC networks as well as late dynamic phases of the T cell-DC interaction.

Symmetry-Breaking Defect Originates in the pSMAC

To understand how PKC θ controls the movement of the T cells during antigen recognition, we compared the zones of the IS to actin cytoskeletal zones common to many types of motile cells. The lamellipodium undergoes contractile oscillations—radial waves that are composed of F-actin-mediated extension and myosin-II-mediated contraction and that move around the perimeter of the contact area—and is thought to be important in mechanical and chemical sensing (Dobereiner et al., 2006; Giannone et al., 2004). Staining of fixed IS showed localization of Arp2/3 and cofilin to the dSMAC and tropomyosin in the pSMAC (Figures S5A and S5B), suggesting that these compartments are similar to the lamellipodium and lamella, respectively, of migrating tissue cells (Gupton et al., 2005; Ponti et al., 2004). We asked whether PKC θ alters contractile oscillations in the dSMAC (Dobereiner et al., 2006). Naive PKC $\theta^{+/+}$ and PKC $\theta^{-/-}$ T cells were fluorescently labeled with the cytoplasmic dye calcein and visualized during contact with planar bilayers. Similar results were obtained with Fab to the dSMAC marker CD45 (data not shown). Time-lapse data on mature IS were then analyzed with an algorithm that tracks the outer edge of the cell contact and measures its instantaneous velocity relative to the cell centroid as a function of position along the roughly circular contact perimeter and time (Figures 4A–4D and Figures S6A–S6D). The velocity maps showed the characteristic “zebra-stripe” pattern of contractile oscillations, with the slight tilt reflecting the speed of the lateral waves (Dobereiner et al., 2006; Giannone et al., 2004) (Figures 4A and 4B). PKC $\theta^{+/+}$ and PKC $\theta^{-/-}$ T cells displayed identical periods of contractile oscillations with an average periodicity of 42 s as determined by power-spectrum anal-

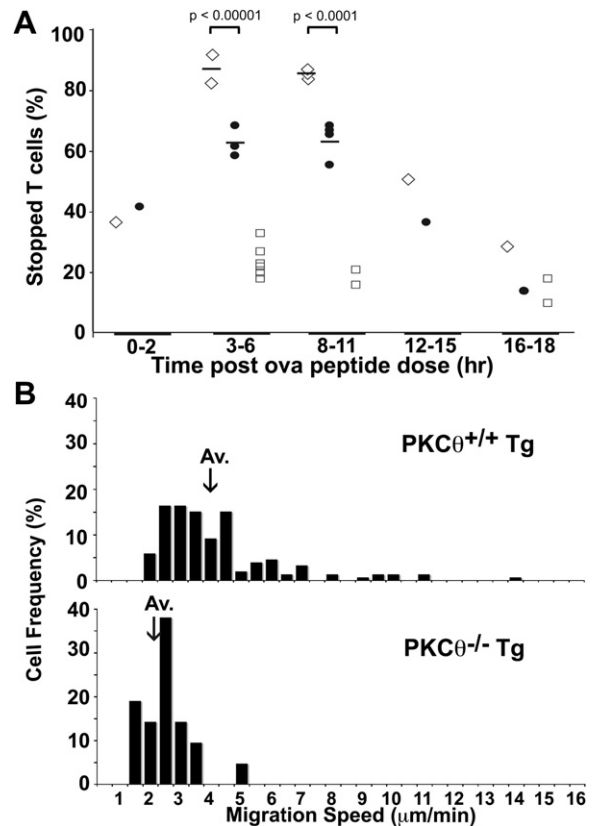


Figure 3. PKC θ Destabilizes the IS In Vivo

(A) Quantification of T cell stopping and breaking the IS in response to peptide in the spleen. DO11.10 PKC $\theta^{-/-}$ (\diamond), DO11.10 PKC $\theta^{+/+}$ (\bullet), and B10D2 PKC $\theta^{+/+}$ (\square) T cells were vitally labeled with combinations of CFSE or CMRA and adoptively transferred to PKC $\theta^{+/+}$ nontransgenic hosts (B10D2). Intravital microscopy of the spleen was performed in various time ranges after peptide injection. Each point represents the percentage of stopped cells in movies with more than 20 cells of each type in the field over 20 min. Black bars represent averages of stopped cells. Shown are p values from Fisher's exact test between PKC $\theta^{+/+}$ DO11.10 and PKC $\theta^{-/-}$ DO11.10 T cells at the same time point.

(B) Speed frequency distribution for one representative field. All cell velocities were measured in the same field to eliminate the effect of spleen movement because of breathing and blood flow. T cell migration speeds were calculated on the same movies where PKC $\theta^{-/-}$ and $\theta^{+/+}$ DO11.10 T cells were transferred into the same host. Speed differences are significant (Mann-Whitney U, $p < 0.001$) and representative of other experiments. Arrows represent the average PKC $\theta^{+/+}$ DO11.10 T cell speed (top graph, 3.93 $\mu\text{m}/\text{min}$) and PKC $\theta^{-/-}$ DO11.10 T cell speed (bottom graph, 2.28 $\mu\text{m}/\text{min}$).

ysis (PKC $\theta^{+/+}$ versus PKC $\theta^{-/-}$, 95% confidence, $p = 0.77$, $F < F_{\text{crit}}$). There was also no difference in the magnitudes of extension and retraction of the cell edge between PKC $\theta^{+/+}$ and PKC $\theta^{-/-}$ T cells. Interestingly, even when PKC $\theta^{+/+}$ T cell were relocating, the contractile oscillations continued to circumnavigate the dSMAC in the migrating cell. Thus, relocating synapses retain a radial lamellipodium-like structure, the dSMAC, and PKC θ does not alter the continuity or symmetry of this extension-retraction process.

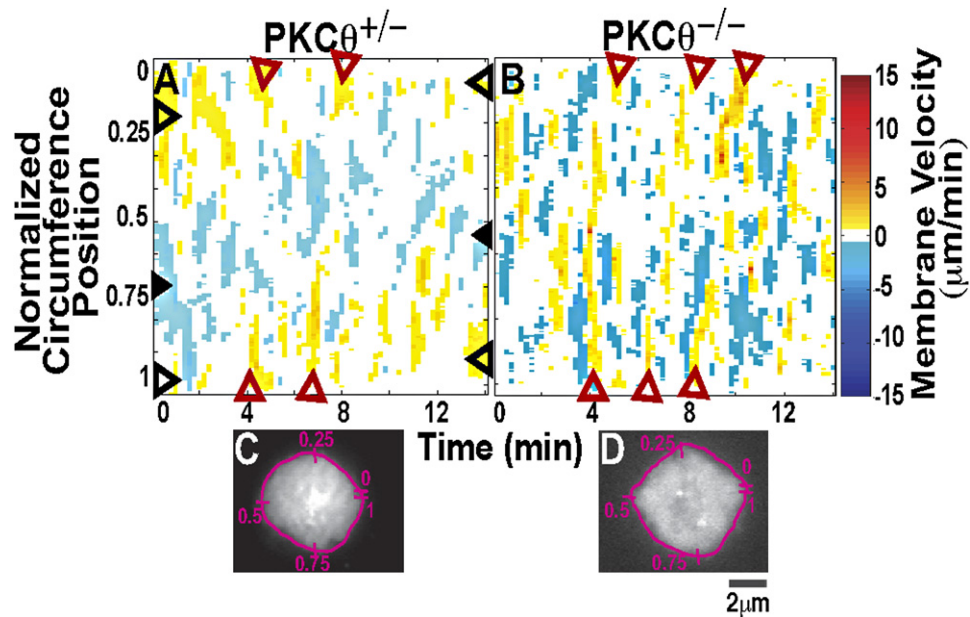


Figure 4. PKC θ and Fast Oscillations in the dSMAC

AND T cells labeled with a cytoplasmic dye were adhered to bilayers containing ICAM-1, CD80, and MHC-peptide complexes and were imaged by TIRFM between 20 and 40 min. Representative maps of membrane velocity as a function of circumference position (equalled to arc length) and time (A and B) are shown, and TIRFM (C and D) images are shown for PKC $\theta^{+/-}$ (A and C) or PKC $\theta^{-/-}$ (B and D) naive CD4 $^{+}$ T cells. The “normalized circumference position” measures relative distance along the roughly circular perimeter counterclockwise from an arbitrary origin. Extensions of greater than $+0.5 \mu\text{m}/\text{min}$ were coded as red/yellow and retractions of greater than $-0.5 \mu\text{m}/\text{min}$ were coded as blue. Velocities below a threshold of $\pm 0.5 \mu\text{m}/\text{min}$ were coded as white. Examples of membrane-extension-velocity banding are shown between open red arrowheads (A and B); membrane-extension-velocity banding resulting from cellular movement is between black open arrowheads; and membrane-retraction-velocity banding resulting from cellular movement is between black filled arrowheads (A). Representations of circumference position are overlaid on the TIRFM images in normalized position values. Horizontal bands correspond to vectorial extension (red) or retraction (blue) that favors movement, and vertical bands correspond to circumferential extension or retraction that favors stable IS. Velocity plots and images correspond to [Movie S9](#) (PKC $\theta^{+/-}$) and [Movie S11](#) (PKC $\theta^{-/-}$). The scale bar represents $2 \mu\text{m}$.

During our time-lapse experiments, we noted that IS relocation in naive T cells resulted from, or was coincident with, a transient loss of symmetry of the pSMAC, which breaks open and forms a crescent or forms more asymmetric focal zones in the direction of movement ([Movies S1 and S2](#)). We quantified this change by measuring the distance between the cSMAC center and the center of the ICAM-1 distribution, which is near zero in a symmetrical IS, but up to $2\text{--}3 \mu\text{m}$ in a relocating cell ([Figure 5](#) and [Table 1](#) [polarity]; see also [Figure S7](#)). Increases in this distance were coincident with speed of relocation. Taken together, our results indicate that PKC θ was required for pSMAC symmetry breaking and relocation but not IS formation or dSMAC dynamics.

WASp $^{-/-}$ T Cell pSMACs Remain Asymmetric: WASp Favors Reforming of the IS after Migration

Breaking the pSMAC could be mediated by an imbalance in contractile forces mediated by myosin II ([Verkhovskiy et al., 1999](#)). It has been shown that a PKC θ -dependent complex of WIP and myosin II is antagonized in a resting NK cell line by WASp ([Krzewski et al., 2006](#)). We investigated the role of WASp in IS symmetry breaking. WASp $^{-/-}$ T cells formed IS; PKC θ was localized to

the pSMAC at 15 min ([Table 1](#) and [Figure 6A](#)). After ~ 20 min, the T cells polarized and laterally migrated as wild-type cells do. However, the WASp $^{-/-}$ T cells did not regain symmetry in the pSMAC to stop IS relocation, thus resulting in sustained asymmetry and faster migration speeds of the naive WASp $^{-/-}$ T cells until they detached from the substrate after ~ 1 hr ([Figures 5B](#) and [6B](#) and [Table 1](#); see also [Movie S13](#)). A small molecule inhibitor of PKC θ ([Cywin et al., 2007](#)) stopped WASp $^{-/-}$ naive T cell relocation, reduced T cell polarity, and restored pSMAC symmetry and stability over 90 min ([Figure 5B](#), bottom, and [Figures 6B](#) and [6C](#); see also [Movie S14](#)). This result is consistent with WASp acting as a negative regulator of a symmetry-breaking process activated by PKC θ . Thus, naive T cells with both PKC θ and WASp activities periodically relocate their IS through reversibly changing the pSMAC to a focal zone, without loss of the dSMAC and cSMAC zones.

DISCUSSION

This study generated a series of surprising findings regarding the nature of the IS during naive T cell activation and regarding the roles of PKC θ and WASp in this

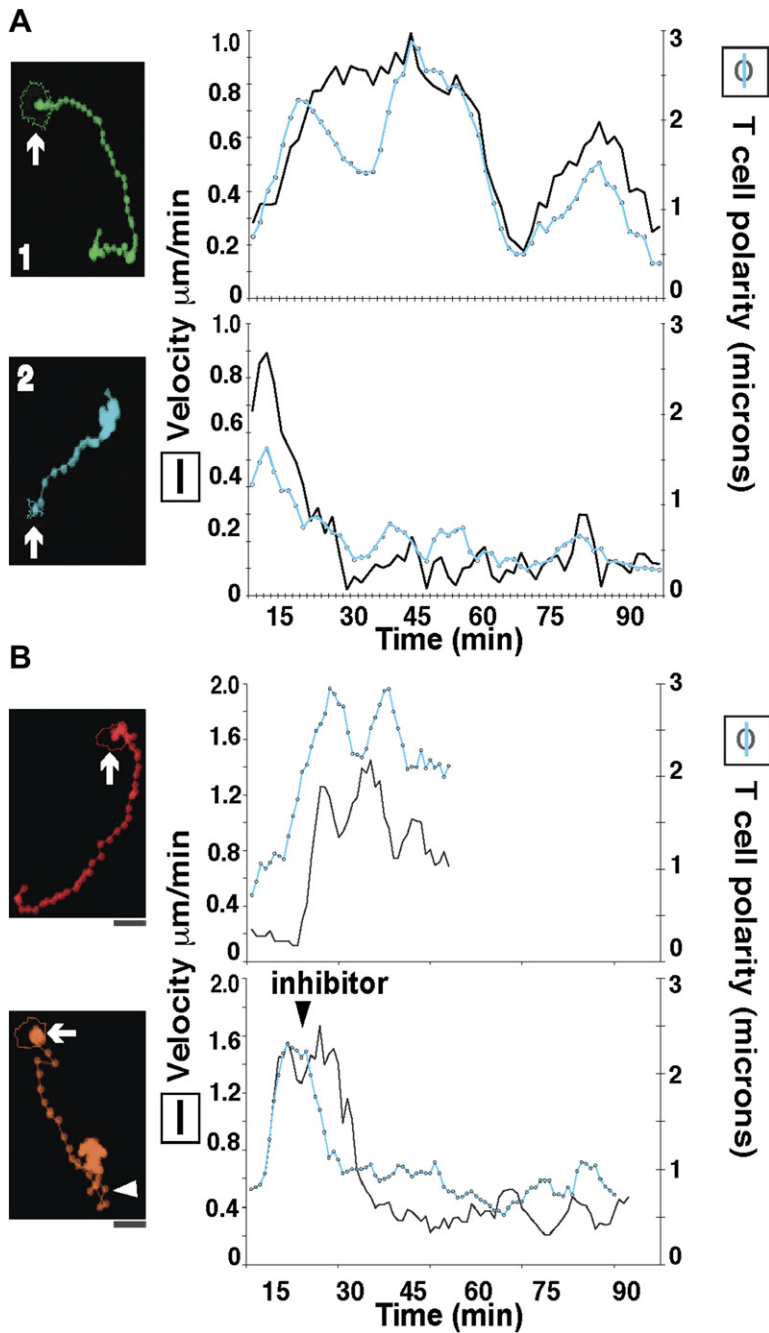


Figure 5. The pSMAC ICAM Ring Undergoes Shape Changes that Correlate with Speed

Naive AND TCR Tg T cells interacted with bilayers and ICAM-1 images were captured every 90 s over 90 min. Cell tracks are shown on the left panel with arrows indicating the starting point. The plot on the right shows the corresponding instantaneous velocity plot and T cell polarity as measured by the distance between the pSMAC and cSMAC centroids (see Supplemental Experimental Procedures, Figures S7 and S9).

(A) Two examples of PKC $\theta^{+/−}$ WASP $^{+/+}$ AND T cells. See Figure S7 for scale.

(B) PKC $\theta^{+/+}$ WASP $^{-/-}$ AND T cells without (top) and with (bottom) PKC θ inhibitor. Inhibitor was added at the time indicated with arrowhead. Pooled data are also summarized in Table 1. The scale bar represents 4 μ m. The PKC $\theta^{+/+}$ WASP $^{-/-}$ AND T cell without inhibitor was followed until it detached from the bilayer.

process. First, PKC θ is not required to form an IS. Second, the ISs of wild-type naive T cells are broken during the first 2 hr after IS formation because of periodic breaks in pSMAC symmetry. Third, PKC θ is required for these breaks in pSMAC symmetry. Fourth, the dSMAC of the IS has markers and dynamics that are lamellipodium like, and the dynamic and radial nature of this structure is retained even when the symmetry of the pSMAC is broken. Fifth, WASp is required for reforming the IS after the initial break in symmetry. Sixth, an inhibitor to PKC θ rescues pSMAC reformation in WASp-deficient T cells.

Finally, T cells that periodically break the symmetry of the IS had a functional advantage over their stable counterparts by making more IL-2. These results change the way we think about IS stability during T cell priming and identify new functions for PKC θ and WASp in control of pSMAC symmetry.

PKC θ has been seen as the prototypical marker of the cSMAC, the central TCR and Lck-rich cluster in the IS (Monks et al., 1998). We have shown that the zones of the naive T cell IS are well reproduced by the supported planar bilayer system including TCR in the cSMAC,

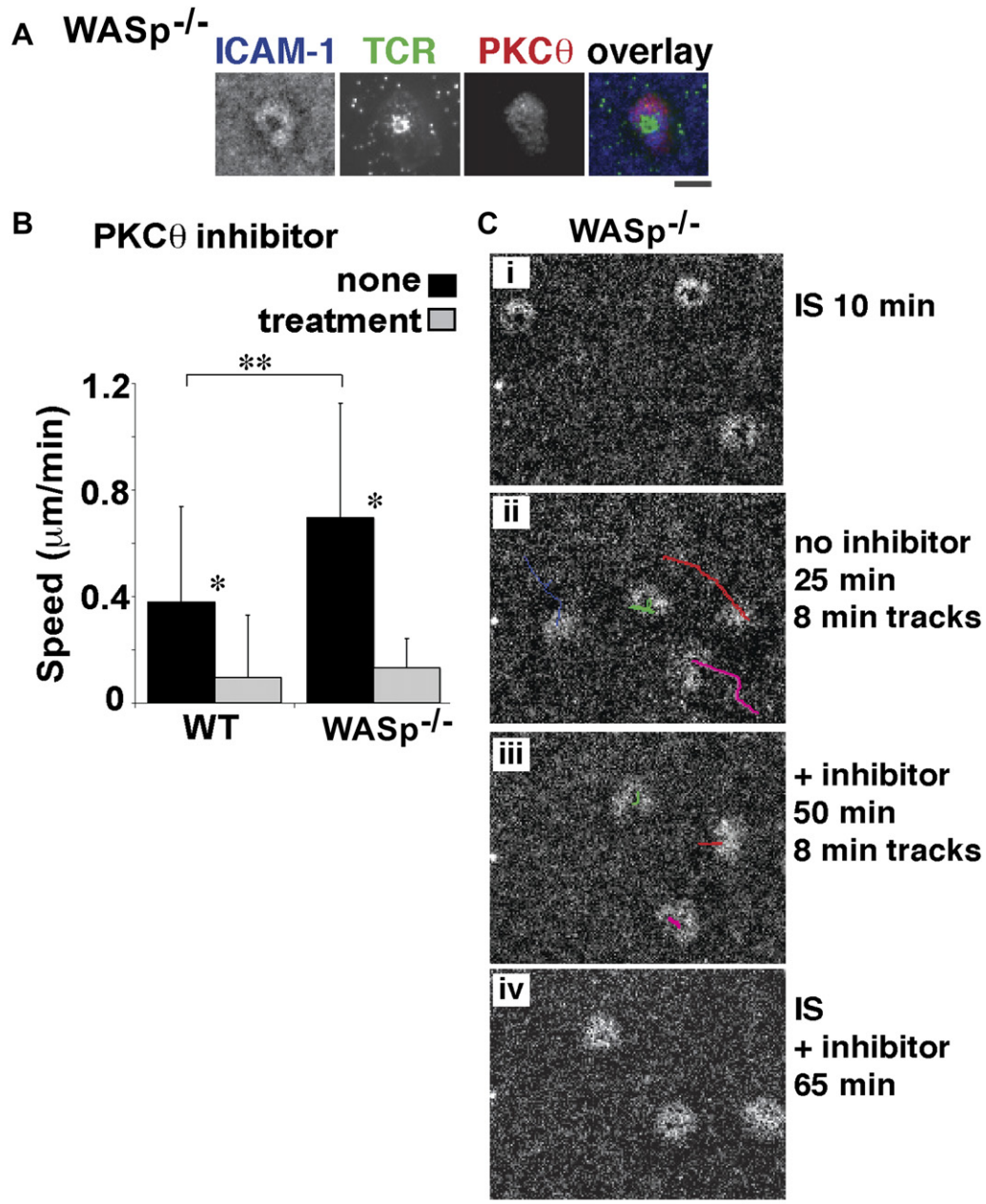


Figure 6. WASp Is Required to Reform the IS

(A) WASp is not required to form the initial IS.

(B) Naive WASp^{+/+} or WASp^{-/-} AND T cells interacted on bilayers for 20 min, and then 1 μM PKC θ inhibitor was added. T cells interacted for another 20 min. The T cell speed was measured, before (none, black bars) and with (treatment, gray bars) the addition of the inhibitor, and averaged. Averages and SD are shown. *t test preinhibitor versus postinhibitor ($p < 0.00001$); **T test WASp^{+/+} versus WASp^{-/-} preinhibitor ($p < 0.00001$).

(C) Images of WASp T cells (i) forming IS, (ii) breaking the IS before treatment with inhibitor, (iii) with inhibitor treatment, and (iv) reforming IS with inhibitor treatment.

ICAM-1 in the pSMAC, and CD45 in the dSMAC, but we found that PKC θ is located in the pSMAC, or the pSMAC/dSMAC junction, rather than the cSMAC. This is not unprecedented in cell-cell systems in that PKC θ has been observed in the pSMAC of T cell-APC junctions (Sanchez-Lockhart et al., 2004). Recently, we have pro-

posed that the cSMAC is largely involved in degradation, whereas signaling is sustained in TCR microclusters in the dSMAC and pSMAC (Varma et al., 2006). Although it was assumed that PKC θ concentrated in the cSMAC is engaged in signaling, it is equally possible that in this location it has been targeted by ubiquitin E3 ligases for

degradation (Heissmeyer et al., 2004). Because we have related PKC θ presence in the pSMAC to symmetry breaking and relocation, a possible strategy to generate highly stable IS in vivo would be to move PKC θ from the pSMAC to the cSMAC. T-B conjugates, in which PKC θ is targeted to the cSMAC, are the most stable T cell-APC ISs in vitro and in vivo (Monks et al., 1998; Okada et al., 2005). Planar bilayers with MHC, ICAM-1, and CD80 lack signals needed to target PKC θ to the cSMAC, which could be further investigated with this system, and display IS relocation similar in magnitude to T cells forming stable interactions with DC in vivo.

The dSMAC appears to play critical roles in sustained signaling by allowing formation of small TCR clusters that are required for sustained signaling (Varma et al., 2006). The generation of dynamic actin in the periphery of model ISs has been shown to require the WAVE2 complex and the cortactin homolog HS-1, both activators of Arp2/3-mediated F-actin polymerization (Gomez et al., 2006; Nolz et al., 2006). Consistent with this, we found that the dSMAC is enriched in F-actin, cofilin, and Arp3. PKC θ is not required for localization of dSMAC/lamellipodial markers (data not shown) or contractile oscillations in the dSMAC, and these contractions require regulated myosin II activity (Giannone et al., 2004). Dynamic actin structures that mediate contractile oscillations in the dSMAC renew T cell-APC contacts to form new TCR microclusters. It remains to be determined whether the dSMAC is essential for TCR microcluster formation or whether alternative mechanisms exist if dSMAC formation is blocked. Contractile oscillations may allow force sensing. T cells may sense the forces exerted by the APC on molecular clusters of MHC-peptide complexes and adhesion molecules that interact with the APC cytoskeleton. This may be analogous to mechanisms used by fibroblasts to sense extracellular matrix rigidity (Giannone et al., 2004). The DC cytoskeleton plays an important role in T cell-APC interactions (Al-Alwan et al., 2001). Consistent with this, barriers to lateral transport of TCR and LFA-1 microclusters in the lipid bilayer containing the MHC-peptide complexes and ICAM-1 enhances TCR-mediated signaling (Mossman et al., 2005).

Helper T cells provide to DCs signals that enhance aspects of the immune response such as CD8 T cell activation and memory (Ridge et al., 1998). Periodic breaking of the symmetrical lamella-like pSMAC to form a polarized focal zone, thus allowing short bursts of migration, may facilitate T cell interaction with multiple DCs (Lindquist et al., 2004). T cells thus may provide critical signals to multiple cells within the local DC network, rather than only one DC as would be the result of a stable IS, to facilitate amplification of the immune response. Because TCR microclusters are formed in the dSMAC, the maintenance of this radial lamellipodial means that relocating T cells can sense antigen-positive APC and compare the newly encountered to the earlier encountered APC (Depoil et al., 2005).

Our intravital-microscopy observations provide insight into the ability of PKC θ -deficient T cells to mount some

types of immune responses in vivo despite profound activation defects in vitro (Marsland et al., 2004). The in vivo environment stimulates very effective PKC θ -independent surveillance of DC networks by naive T cells. This suggests that PKC θ is not required to respond to chemotactic and chemokinetic signals associated with secondary lymphoid tissues, consistent with the normal cellularity of these tissues in PKC $\theta^{-/-}$ mice (Sun et al., 2000). The in vivo difference between PKC $\theta^{+/+}$ and PKC $\theta^{-/-}$ T cells we detected was greater positional stability at 3–8 hr after antigen exposure, and this is likely to correspond to greater IS stability. The destabilized IS speed in vivo ($\sim 4 \mu\text{m}/\text{min}$) is intermediate between accepted speeds for arrest ($< 2 \mu\text{m}/\text{min}$) and free migration ($> 6 \mu\text{m}/\text{min}$) and falls in the same range as the long-term T-DC conjugate interactions ($\sim 2\text{--}5 \mu\text{m}/\text{min}$) (Mempel et al., 2004). The major phenotypic defect in PKC θ -deficient mice in vivo is the failure to make Th2 responses in the context of allergic airway reactivity and parasitic-infection models (Marsland et al., 2004; Salek-Ardakani et al., 2004). Interestingly, T cells from WASp-deficient patients, cells that also have some function in vivo, have been shown to have defects in producing Th1 cytokines (Trifari et al., 2006). Thus, stable IS may be important for Th1 responses, whereas the ability to relocate IS may be important for Th2 responses. The reformation of IS favored by WASp may regulate T cell differentiation by promoting asymmetric cell divisions (Dustin and Chan, 2000). Recently, Chang et al. have found that ISs lead to asymmetric cell divisions important for memory/effector differentiation (Chang et al., 2007).

We have described the autonomous relocation of naive T cell ISs and provided genetic evidence for a control pathway. First, we show that PKC θ allows T cells to break the symmetry of the pSMAC, thus promoting slow migration via an asymmetric LFA-1 focal zone (lamella) (Smith et al., 2005). Interestingly, this symmetry breaking is restricted to the pSMAC because the dSMAC appears to retain radial symmetry as reflected in contractile oscillations. Then we show that WASp allows T cells to reform their IS by re-establishing a symmetric pSMAC. Furthermore, pSMAC re-establishment in WASp-deficient T cells can be rescued by inhibition of PKC θ with a selective inhibitor. A biochemical framework for our results is provided by a recent study in NK cells where it was shown that cell activation allowed PKC θ -mediated WIP association that is independent of WASp with myosin IIA. Although these interactions were important for NK cell function, their specific role in control of the NK cell IS was not explored. We have found PKC θ in the integrin-rich pSMAC, where it is well positioned to control tension in the F-actin network leading to periodic “tearing open” of the ring to generate an asymmetric focal zone (Smith et al., 2005; Verkhovskiy et al., 1999). We speculate that inhibition of myosin IIA by WASp inclusion in this complex may allow the symmetric pSMAC to reform after a period of relocation. Along these lines, previously activated PKC $\theta^{+/+}$ T cells migrate 2- to 3-fold more quickly than PKC $\theta^{-/-}$ T cells on ICAM-1 substrates (data not shown).

This is consistent with PKC θ boosting lamellar traction forces through a myosin-II-dependent process (Pollard and Borisy, 2003). The immunological synapse provides a new model for genetic control of symmetry breaking and reestablishment, a model that has direct implications for T cell and NK cell function.

EXPERIMENTAL PROCEDURES

T Cell Purification

PKC $\theta^{-/-}$ and WASP $^{-/-}$ mice have been described elsewhere (Snapper et al., 1998; Sun et al., 2000). PKC $\theta^{-/-}$ were backcrossed to B6 for 15 generations and to B10D2 for ten generations. PKC $\theta^{-/-}$ and WASP $^{-/-}$ B6 mice were crossed onto AND TCR transgenic mice. DO11.10 TCR transgenic mice with the B10D2.PKC $\theta^{-/-}$ were used in these antigen specific *in vivo* experiments. Naive CD4 $^{+}$ T cells from lymph nodes and spleens were negatively purified with magnetic beads (Miltenyi Biotech).

Bilayers

Bilayers preparation has been described in detail elsewhere. In brief, mouse ICAM-1 with a glycosylphosphatidylinositol anchor (ICAM-1-GPI) labeled with Cy5 (Grakoui et al., 1999) and I-E k was purified from transfected CHO cells and labeled with Oregon Green (OG) and loaded with MCC peptide. All data shown are at an I-E k -MCC density of 10 molecules/ μm^2 . Mouse CD80 with a glycosylphosphatidylinositol anchor (CD80-GPI) was also used. See the [Supplemental Data](#).

T Cell Electroporation

Naive lymph-node cells were electroporated in accordance with Amara protocols. The PKC θ -yfp construct was purified with endotoxin-free conditions (Qiagen). Cells were used after 6 hr of incubation.

Reagents and Staining

The PKC θ inhibitor (compound #20) was kindly provided by Boehringer-Ingelheim Pharmaceuticals, Inc. (Cywin et al., 2007). It was dissolved in DMSO (0.1% final concentration) and did not inhibit ICAM-1 accumulation, phosphotyrosine staining, or lamellipodium-like extension formation under the same conditions as it inhibited migration (Figure S8). DMSO alone did not change migration (t test, instantaneous speed of naive T cells treated with or without DMSO, $p = 0.11$).

Cytokine-secretion assays were performed with the Miltenyi Biotec IL2 capture assay, in accordance with the manufacturer's instructions with the following changes: T cells were allowed to interact with bilayers at 37°C for 15 min, were washed, and then were stained with the capture reagent for 10 min and washed again. Cells interacted with the bilayers and were imaged hourly for 4 or 6 hr and then were stained with the IL2 detection reagent for 10 min. The cells were imaged immediately after washing. Measurements of the plasma membrane were taken for quantitation.

For staining the T cell-bilayer interface, cells interacted with the bilayers for 30 min to 2 hr in imaging buffer. Cells were fixed with 2% PFA, permeabilized with 0.05% Triton-X 100, and blocked in 100 $\mu\text{g}/\text{ml}$ goat IgG in imaging buffer. Cells were incubated with rabbit polyclonal anti-PKC θ (Santa Cruz, sc-212), mouse monoclonal anti-talin (Sigma, T3287), rabbit polyclonal anti-cofilin (Cytoskeleton, ACFL02), mouse monoclonal anti-TM (Sigma, T2780), sheep polyclonal anti-Arp3 (Cytoskeleton, AAR01), or biotinylated anti-phosphotyrosine (4G10, Upstate Biotechnology) and then incubated with fluorescently tagged goat anti-rabbit Fab $_2$ (Molecular Probes, A-11071), goat anti-mouse Fab $_2$ (Molecular Probes, A-11018), donkey anti-sheep IgG (Molecular Probes, A-21099), or avidin (Molecular Probes, A-21370) that were used as secondary reagents. F-actin was stained with phalloidin conjugated with Alexa 488 (Molecular Probes, A12379). For PKC θ staining, this combination gave specific staining 14-fold greater in PKC $\theta^{+/+}$ T cells than in PKC $\theta^{-/-}$ T cells. Secondary staining only in PKC $\theta^{+/+}$ cells

was 10-fold reduced than the primary-secondary combination. Contacts were imaged for staining by total internal-reflection microscopy (TIRFM). TCR and CD45 were visualized with fluorescently labeled monovalent Fab fragments (H57 and I3/2.3, respectively). Latrunculin A was used at 1 μM (Sigma-Aldrich, L5163).

Microscopy and Image Analysis

An inverted wide-field microscope with cooled CCD camera (Yona Microscopes) was used for multicolor fluorescence, interference reflection microscopy (Grakoui et al., 1999), and TIRFM. A Zeiss LSM 510 confocal microscope (Carl Zeiss) was used for intravital microscopy. Image processing and bilayer calibration were performed with IP-Lab (Scanalytics), Metamorph (Molecular Devices), Image J, or Velocity (Improvision) software.

Morphology Analysis

Cells on bilayers were analyzed for morphology changes with Metamorph and Image J. The centroid of the mass of ICAM-1 accumulation and then the continuous outer boundary of fluorescence intensity were found with Metamorph (pSMAC). ICAM-1 exclusion centroids (cSMAC) were tracked in Image J. The distance between the cSMAC and pSMAC (Figure S9) was plotted. For the average instantaneous velocity plot and cSMAC-pSMAC distances, the rolling average of five frames was plotted for each time point.

Long-Term IS Stability

Naive PKC $\theta^{+/+}$ or PKC $\theta^{+/-}$ and PKC $\theta^{-/-}$ AND TCR transgenic (Tg) cells from littermates were vitally labeled with CFSE or CMRA (or one genotype was left unlabeled), mixed together in combinations, and allowed to interact with bilayers for 4 hr at 37°C. Nonadherent cells were washed. Cells in 8–12 fields were imaged hourly from 30–180 min. The nonmotile population of cells was tracked frame by frame for each genotype, and ISs were scored as stable if they stayed within one cell diameter of their original location at 30 min. Specifically, we recorded the initial IS position after 30 min of IS formation and considered the IS stable if it remained within 10 μm of its initial position over one hour. These experiments were repeated with PKC $\theta^{+/-}$ or PKC $\theta^{+/+}$ and PKC $\theta^{-/-}$ 2B4 and 5CC7 TCR Tg cells and similar results were found. Mice were matched for their TCR Tg expression levels.

Intravital Microscopy

B10D2 mice were injected IV with combinations of PKC $\theta^{-/-}$ and PKC $\theta^{+/+}$ DO11.10 TCR Tg and B10D2 purified naive T cells that were vitally labeled (Molecular Probes). Mice were left untreated or were injected with ovalbumin peptide. Spleens were exposed for intravital-imaging analysis. Animals were maintained at 37°C and on O $_2$ throughout imaging. T cells were scored as stopped if they remained within three cell diameters of their original location from the start of image acquisition to 20 min. More details are provided in the [Supplemental Data](#).

Membrane Dynamics

CD4 $^{+}$ naive T cells were purified from littermate AND PKC $\theta^{-/-}$ or PKC $\theta^{+/+}$ mice and incubated on bilayers containing ICAM-1-Cy5 and unlabeled I-E k and CD80. Cells were vitally labeled with the cytoplasmic fluorescent dye Calcein AM (Molecular Probes), and images of contacts were acquired by TIRFM every 3 or 12 s for ~ 15 min. For velocity calculations, see the [Supplemental Data](#).

Supplemental Data

Supplemental Data includes additional Experimental Procedures, nine figures, and fourteen movies and can be found with this article online at <http://www.cell.com/cgi/content/full/129/4/773/DC1/>.

ACKNOWLEDGMENTS

We thank M. Nussenzweig for the CD11c⁺-YFP mice; and V. Nussenzweig for the WASp^{-/-} mice; H.-G. Doeberiner, M. Brown, P. Ohashi and A. Douglass for helpful discussion; and T. Starr, T. Wu, and H. Patel for technical assistance. T.N.S. was supported in part through a National Psoriasis Foundation/USA seed grant and a National Institute of Allergy and Infectious Diseases (NIAID) AIDS Institutional Training Grant. T.J.S. was supported by a NIAID AIDS Institutional Training Grant. R.V. was supported by a Bernard Levine Fellowship. M.P.S., D.R.L. and M.L.D. were supported by the National Institutes of Health. M.L.D. was supported by the Irene Diamond Foundation. D.R.L. is an investigator of the Howard Hughes Medical Institute.

Received: January 6, 2006

Revised: January 18, 2007

Accepted: March 23, 2007

Published: May 17, 2007

REFERENCES

- Al-Alwan, M.M., Rowden, G., Lee, T.D., and West, K.A. (2001). The dendritic cell cytoskeleton is critical for the formation of the immunological synapse. *J. Immunol.* **166**, 1452–1456.
- Badour, K., Zhang, J., Shi, F., McGavin, M.K., Rampersad, V., Hardy, L.A., Field, D., and Siminovitch, K.A. (2003). The Wiskott-Aldrich syndrome protein acts downstream of CD2 and the CD2AP and PSTPIP1 adaptors to promote formation of the immunological synapse. *Immunity* **18**, 141–154.
- Berg-Brown, N.N., Gronski, M.A., Jones, R.G., Elford, A.R., Deenick, E.K., Odermatt, B., Littman, D.R., and Ohashi, P.S. (2004). PKC θ signals activation versus tolerance in vivo. *J. Exp. Med.* **199**, 743–752.
- Bromley, S.K., laboni, A., Davis, S.J., Whitty, A., Green, J.M., Shaw, A.S., Weiss, A., and Dustin, M.L. (2001). The immunological synapse and CD28–CD80 interactions. *Nat. Immunol.* **2**, 1159–1166.
- Bubeck Wardenburg, J., Pappu, R., Bu, J.Y., Mayer, B., Chernoff, J., Straus, D., and Chan, A.C. (1998). Regulation of PAK activation and the T cell cytoskeleton by the linker protein SLP-76. *Immunity* **9**, 607–616.
- Calle, Y., Jones, G.E., Jagger, C., Fuller, K., Blundell, M.P., Chow, J., Chambers, T., and Thrasher, A.J. (2004). WASp deficiency in mice results in failure to form osteoclast sealing zones and defects in bone resorption. *Blood* **103**, 3552–3561.
- Cannon, J.L., and Burkhardt, J.K. (2004). Differential roles for Wiskott-Aldrich syndrome protein in immune synapse formation and IL-2 production. *J. Immunol.* **173**, 1658–1662.
- Chang, J.T., Palanivel, V.R., Kinjyo, I., Shambach, F., Intlekofer, A.M., Banerjee, A., Longworth, S.A., Vinup, K.E., Mrass, P., Oliaro, J., et al. (2007). Asymmetric T lymphocyte division in the initiation of adaptive immune responses. *Science* **315**, 1687–1691.
- Cywin, C.L., Dahmann, G., Prokopowicz, A.S., 3rd, Young, E.R., Magolda, R.L., Cardozo, M.G., Cogan, D.A., Disalvo, D., Ginn, J.D., Kashem, M.A., et al. (2007). Discovery of potent and selective PKC θ inhibitors. *Bioorg. Med. Chem. Lett.* **17**, 225–230.
- Depoil, D., Zaru, R., Guiraud, M., Chauveau, A., Harriague, J., Bismuth, G., Utzny, C., Muller, S., and Valitutti, S. (2005). Immunological synapses are versatile structures enabling selective T cell polarization. *Immunity* **22**, 185–194.
- Dobereiner, H.G., Dubin-Thaler, B.J., Hofman, J.M., Xenias, H.S., Sims, T.N., Giannone, G., Dustin, M.L., Wiggins, C.H., and Sheetz, M.P. (2006). Lateral membrane waves constitute a universal dynamic pattern of motile cells. *Phys. Rev. Lett.* **97**, 038102.
- Douglass, A.D., and Vale, R.D. (2005). Single-molecule microscopy reveals plasma membrane microdomains created by protein-protein networks that exclude or trap signaling molecules in T cells. *Cell* **121**, 937–950.
- Dustin, M.L., and Chan, A.C. (2000). Signaling takes shape in the immune system. *Cell* **103**, 283–294.
- Freiberg, B.A., Kupfer, H., Maslanik, W., Delli, J., Kappler, J., Zaller, D.M., and Kupfer, A. (2002). Staging and resetting T cell activation in SMACs. *Nat. Immunol.* **3**, 911–917.
- Giannone, G., Dubin-Thaler, B.J., Dobereiner, H.G., Kieffer, N., Bresnick, A.R., and Sheetz, M.P. (2004). Periodic lamellipodial contractions correlate with rearward actin waves. *Cell* **116**, 431–443.
- Gomez, T.S., McCarney, S.D., Carrizosa, E., Labno, C.M., Comiskey, E.O., Nolz, J.C., Zhu, P., Freedman, B.D., Clark, M.R., Rawlings, D.J., et al. (2006). HS1 functions as an essential actin-regulatory adaptor protein at the immune synapse. *Immunity* **24**, 741–752.
- Grakoui, A., Bromley, S.K., Sumen, C., Davis, M.M., Shaw, A.S., Allen, P.M., and Dustin, M.L. (1999). The immunological synapse: A molecular machine controlling T cell activation. *Science* **285**, 221–227.
- Gupton, S.L., Anderson, K.L., Kole, T.P., Fischer, R.S., Ponti, A., Hitchcock-DeGregori, S.E., Danuser, G., Fowler, V.M., Wirtz, D., Hanein, D., and Waterman-Storer, C.M. (2005). Cell migration without a lamellipodium: Translation of actin dynamics into cell movement mediated by tropomyosin. *J. Cell Biol.* **168**, 619–631.
- Heissmeyer, V., Macian, F., Im, S.H., Varma, R., Feske, S., Venuprasad, K., Gu, H., Liu, Y.C., Dustin, M.L., and Rao, A. (2004). Calcineurin imposes T cell unresponsiveness through targeted proteolysis of signaling proteins. *Nat. Immunol.* **5**, 255–265.
- Kraal, G., Breel, M., Janse, M., and Bruin, G. (1986). Langerhans' cells, veiled cells, and interdigitating cells in the mouse recognized by a monoclonal antibody. *J. Exp. Med.* **163**, 981–997.
- Krzewski, K., Chen, X., Orange, J.S., and Strominger, J.L. (2006). Formation of a WIP-, WASp-, actin-, and myosin IIA-containing multi-protein complex in activated NK cells and its alteration by KIR inhibitory signaling. *J. Cell Biol.* **173**, 121–132.
- Kucik, D.F., Dustin, M.L., Miller, J.M., and Brown, E.J. (1996). Adhesion-activating phorbol ester increases the mobility of leukocyte integrin LFA-1 in cultured lymphocytes. *J. Clin. Invest.* **97**, 2139–2144.
- Lin, C.H., Espreafico, E.M., Mooseker, M.S., and Forscher, P. (1996). Myosin drives retrograde F-actin flow in neuronal growth cones. *Neuron* **16**, 769–782.
- Lindquist, R.L., Shakhar, G., Dudziak, D., Wardemann, H., Eisenreich, T., Dustin, M.L., and Nussenzweig, M.C. (2004). Visualizing dendritic cell networks in vivo. *Nat. Immunol.* **5**, 1243–1250.
- Marsland, B.J., Soos, T.J., Spath, G., Littman, D.R., and Kopf, M. (2004). Protein kinase C θ is critical for the development of in vivo T helper (Th)2 cell but not Th1 cell responses. *J. Exp. Med.* **200**, 181–189.
- Mempel, T.R., Henrickson, S.E., and Von Andrian, U.H. (2004). T-cell priming by dendritic cells in lymph nodes occurs in three distinct phases. *Nature* **427**, 154–159.
- Miller, M.J., Wei, S.H., Cahalan, M.D., and Parker, I. (2003). Autonomous T cell trafficking examined in vivo with intravital two-photon microscopy. *Proc. Natl. Acad. Sci. USA* **100**, 2604–2609.
- Monks, C.R., Freiberg, B.A., Kupfer, H., Sciaky, N., and Kupfer, A. (1998). Three-dimensional segregation of supramolecular activation clusters in T cells. *Nature* **395**, 82–86.
- Monks, C.R., Kupfer, H., Tamir, I., Barlow, A., and Kupfer, A. (1997). Selective modulation of protein kinase C- θ during T-cell activation. *Nature* **385**, 83–86.
- Mossman, K.D., Campi, G., Groves, J.T., and Dustin, M.L. (2005). Altered TCR signaling from geometrically repatterned immunological synapses. *Science* **310**, 1191–1193.
- Nolz, J.C., Gomez, T.S., Zhu, P., Li, S., Medeiros, R.B., Shimizu, Y., Burkhardt, J.K., Freedman, B.D., and Billadeau, D.D. (2006). The

- WAVE2 complex regulates actin cytoskeletal reorganization and CRAC-mediated calcium entry during T cell activation. *Curr. Biol.* 16, 24–34.
- Okada, T., Miller, M.J., Parker, I., Krummel, M.F., Neighbors, M., Hartley, S.B., O'Garra, A., Cahalan, M.D., and Cyster, J.G. (2005). Antigen-engaged B cells undergo chemotaxis toward the T zone and form motile conjugates with helper T cells. *PLoS Biol.* 3, e150.
- Pollard, T.D., and Borisy, G.G. (2003). Cellular motility driven by assembly and disassembly of actin filaments. *Cell* 112, 453–465.
- Ponti, A., Machacek, M., Gupton, S.L., Waterman-Storer, C.M., and Danuser, G. (2004). Two distinct actin networks drive the protrusion of migrating cells. *Science* 305, 1782–1786.
- Ridge, J.P., Di Rosa, F., and Matzinger, P. (1998). A conditioned dendritic cell can be a temporal bridge between a CD4⁺ T-helper and a T-killer cell. *Nature* 393, 474–478.
- Salek-Ardakani, S., So, T., Halteman, B.S., Altman, A., and Croft, M. (2004). Differential regulation of Th2 and Th1 lung inflammatory responses by protein kinase C theta. *J. Immunol.* 173, 6440–6447.
- Sanchez-Lockhart, M., Marin, E., Graf, B., Abe, R., Harada, Y., Sedwick, C.E., and Miller, J. (2004). Cutting edge: CD28-mediated transcriptional and posttranscriptional regulation of IL-2 expression are controlled through different signaling pathways. *J. Immunol.* 173, 7120–7124.
- Sasahara, Y., Rachid, R., Byrne, M.J., de la Fuente, M.A., Abraham, R.T., Ramesh, N., and Geha, R.S. (2002). Mechanism of recruitment of WASP to the immunological synapse and of its activation following TCR ligation. *Mol. Cell* 10, 1269–1281.
- Sevilla, N., Kunz, S., McGavern, D., and Oldstone, M.B. (2003). Infection of dendritic cells by lymphocytic choriomeningitis virus. *Curr. Top. Microbiol. Immunol.* 276, 125–144.
- Shakhar, G., Lindquist, R.L., Skokos, D., Dudziak, D., Huang, J.H., Nussenzweig, M.C., and Dustin, M.L. (2005). Stable T cell-dendritic cell interactions precede the development of both tolerance and immunity in vivo. *Nat. Immunol.* 6, 707–714.
- Smith, A., Carrasco, Y.R., Stanley, P., Kieffer, N., Batista, F.D., and Hogg, N. (2005). A talin-dependent LFA-1 focal zone is formed by rapidly migrating T lymphocytes. *J. Cell Biol.* 170, 141–151.
- Snapper, S.B., Rosen, F.S., Mizoguchi, E., Cohen, P., Khan, W., Liu, C.H., Hagemann, T.L., Kwan, S.P., Ferrini, R., Davidson, L., et al. (1998). Wiskott-Aldrich syndrome protein-deficient mice reveal a role for WASP in T but not B cell activation. *Immunity* 9, 81–91.
- Somersalo, K., Anikeeva, N., Sims, T.N., Thomas, V.K., Strong, R.K., Spies, T., Lebedeva, T., Sykulev, Y., and Dustin, M.L. (2004). Cytotoxic T lymphocytes form an antigen-independent ring junction. *J. Clin. Invest.* 113, 49–57.
- Stinchcombe, J.C., Majorovits, E., Bossi, G., Fuller, S., and Griffiths, G.M. (2006). Centrosome polarization delivers secretory granules to the immunological synapse. *Nature* 443, 462–465.
- Sun, Z., Arendt, C.W., Ellmeier, W., Schaeffer, E.M., Sunshine, M.J., Gandhi, L., Annes, J., Petrzilka, D., Kupfer, A., Schwartzberg, P.L., and Littman, D.R. (2000). PKC-theta is required for TCR-induced NF-kappaB activation in mature but not immature T lymphocytes. *Nature* 404, 402–407.
- Thome, M. (2003). The immunological synapse and actin assembly: A regulatory role for PKC theta. *Dev. Cell* 4, 3–5.
- Trifari, S., Sitia, G., Aiuti, A., Scaramuzza, S., Marangoni, F., Guidotti, L.G., Martino, S., Saracco, P., Notarangelo, L.D., Roncarolo, M.G., and Dupre, L. (2006). Defective Th1 cytokine gene transcription in CD4⁺ and CD8⁺ T cells from Wiskott-Aldrich syndrome patients. *J. Immunol.* 177, 7451–7461.
- Valitutti, S., Dessing, M., Aktories, K., Gallati, H., and Lanzavecchia, A. (1995). Sustained signaling leading to T cell activation results from prolonged T cell receptor occupancy. Role of T cell actin cytoskeleton. *J. Exp. Med.* 181, 577–584.
- Varma, R., Campi, G., Yokosuka, T., Saito, T., and Dustin, M.L. (2006). T cell receptor-proximal signals are sustained in peripheral microclusters and terminated in the central supramolecular activation cluster. *Immunity* 25, 117–127.
- Verkhovskiy, A.B., Svitkina, T.M., and Borisy, G.G. (1999). Self-polarization and directional motility of cytoplasm. *Curr. Biol.* 9, 11–20.
- Villalba, M., Bi, K., Hu, J., Altman, Y., Bushway, P., Reits, E., Neefjes, J., Baier, G., Abraham, R.T., and Altman, A. (2002). Translocation of PKC[theta] in T cells is mediated by a nonconventional, PI3-K- and Vav-dependent pathway, but does not absolutely require phospholipase C. *J. Cell Biol.* 157, 253–263.
- Zell, T., Khoruts, A., Ingulli, E., Bonnevier, J.L., Mueller, D.L., and Jenkins, M.K. (2001). Single-cell analysis of signal transduction in CD4 T cells stimulated by antigen in vivo. *Proc. Natl. Acad. Sci. USA* 98, 10805–10810.